9.8 Receiver with Integrated Magnetic-Free N-Path-Filter-Based Non-Reciprocal Circulator and Baseband Self-Interference Cancellation for Full-Duplex Wireless

Jin Zhou, Negar Reiskarimian , Harish Krishnaswamy

Columbia University, New York, NY

Full-duplex (FD) is an emergent wireless communication paradigm where the transmitter (TX) and the receiver (RX) operate at the same time and at the same frequency. The fundamental challenge with FD is the tremendous amount of TX self-interference (SI) at the RX. Low-power applications relax FD system requirements [1], but an FD system with -6dBm transmit power, 10MHz signal bandwidth and 12dB NF budget still requires 86dB of SI suppression to reach the -92dBm noise floor. Recent research has focused on techniques for integrated self-interference cancellation (SIC) in FD receivers [1-3]. Open challenges include achieving the challenging levels of SIC through multi-domain cancellation, and low-loss shared-antenna (ANT) interfaces with high TX-to-RX isolation. Shared-antenna interfaces enable compact form factor, translate easily to MIMO, and ease system design through channel reciprocity.

In this paper, we present an FD receiver with an integrated magnetic-free N-path-filter-based circulator and analog baseband (BB) SI cancellation (Fig. 9.8.1). This FD receiver (1) enables a compact FD radio with an integrated shared-antenna interface, (2) achieves 42dB on-chip SI suppression across antenna and analog BB domains over a 12MHz signal BW, and (3) in conjunction with digital SI and its IM3 distortion cancellation, demonstrates 85dB overall SI suppression, enabling an FD link budget of –7dBm TX average output power and –92dBm noise floor.

Linear time-invariant (LTI) passive systems based on conventional materials are *reciprocal* under the Lorentz Reciprocity Theorem. *A three-port, matched, reciprocal network cannot be lossless*. Consequently, a three-port antenna interface with high TX-RX isolation, such as electrical balance duplexers [4], *necessarily features at least 3dB loss (typically 4dB) between TX-ANT and ANT-RX*. Non-reciprocal circulators avoid this fundamental 3dB loss, but rely on magnetic materials, and cannot be integrated on silicon. However, *linear time-varying (LTV) systems can be non-reciprocal*. Two-port N-path filters with a phase-shift between the input and output clocks have been explored as a means of adding phase shift to signals traveling through the filter [2]. *Interestingly, the phase-shifts applied to signals near the switching frequency traveling in opposite directions have opposite signs* (Fig. 9.8.2) – the magnitudes of S_{21} and S_{12} are equal (and exhibit low loss for large N) but the phases of S_{21} and S_{12} are opposite in sign and equal in magnitude to the clock phase shift. This non-reciprocal phase response can be verified through LPTV analysis. The theoretical S parameters of such a two-port N-path filter at the switching frequency are given in Fig. 9.8.2 assuming a large N-path RC time-constant, along with an approximation for large N. This behavior can also be understood by viewing the two switch sets as reciprocal quadrature mixers. The capacitors act as a lowpass filter that attenuates the upconverted signal from the first mixer in either propagation direction. The phase-shifted LO performs upconversion in one direction but downconversion in the other, resulting in non-reciprocal phase response.

To create non-reciprocal wave propagation, a $3\lambda/4$ transmission line is wrapped around the N-path filter with +90° clock phase shift. *In such a ring, signals can only propagate in one direction*. In the clockwise direction in Fig. 9.8.2, the -270° phase shift of the $3\lambda/4$ line combines with the -90° shift of the N-path filter to create constructive interference. Counter-clockwise, the -270° shift of the line adds with the +90° shift of the N-path to create destructive interference.

A three-port circulator can be realized by introducing three ports anywhere on the transmission line, as long as they maintain a $\lambda/4$ circumferential distance between them. Figure 9.8.3 shows the resultant 3-port S-parameter matrix for large N, which matches that of an ideal circulator. However, if the RX port is placed next to the N-path filter (l=0 in Fig. 9.8.3), then for TX port excitations, the RX port, and hence one end of the N-path filter, is quiet due to the isolation of the circulator. The S-parameters of the non-reciprocal N-path filter force its two port voltages to be equal in magnitude, and consequently, *its other end is quiet as well. In other words, voltage swings across the N-path filter are suppressed, resulting in high linearity to excitations at the TX port*.

Yet another interesting feature is that this circulator can be reconfigured to operate as a half-duplex (TDD) T/R switch. If the clock drive is cut and the switches are left open, the circulator simply becomes a low-loss 50Ω transmission line from ANT to RX. Similarly, the circulator reduces to a low-loss 50Ω line from ANT to TX if a pair of switches is held high.

The circulator was designed for tunable operation around 750MHz in 65nm CMOS. The $3\lambda/4$ line is miniaturized using three CLC networks, with the inductors placed off-chip (Figs. 9.8.1 and 9.8.3). 8 paths are used in the N-path filter to lower the loss. Clock phase shifting is accomplished using vector-interpolation phase shifters (Fig. 9.8.1). The circulator is integrated with a noise-canceling current-mode RX. Both circulator and RX are powered from 1.2V supplies. SIC at the analog baseband (BB) is required to further relax the RX and ADC dynamic range requirements, especially under a high RX gain. The analog BB canceller taps from the TX BB, adjusts the amplitude and the phase, and injects the cancellation current at the TIA input (Fig. 9.8.1). Performing BB SIC at the TIA input not only protects the RX analog BB circuits, but also enhances the RX mixer and LNTA linearity by creating a virtual ground at the passive mixer output. Amplitude and phase scaling is achieved through two 5b vector-modulators (VM) injecting into the I- and Q-paths of the RX analog BB. Each VM consists of 31 identical cells with independent controls, similar to [1]. The unit cell of the VM adopts a noise-canceling common-gate (CG) and common-source (CS) topology, allowing the partial cancellation of the noise from the CG devices (dependent on the VM setting). 1.3V and 2.2V supplies are used for the BB canceler (in Fig. 9.8.1).

Measurements from a breakout of the circulator in FD mode reveal 1.7dB loss in TX-ANT and ANT-RX transmission and broadband isolation better than 15dB between TX and RX (the narrowband isolation can be as high as 50dB). The in-band ANT-RX IIP3 is +8.7dBm while the in-band TX-ANT IIP3 is +27.5dBm, significantly higher due to the suppression of swing across the N-path filter. The ANT-RX NF is 4.3dB, degraded from the expected 2dB NF due to LO-path phase noise. Elimination of the phase shifters (not necessary as only a static 90° phase shift is desired) restores the NF to around 2dB in simulation. The receiver with the integrated circulator and analog BB SIC (Figs. 9.8.1 and 9.8.7) operates over 0.6 to 0.8GHz, with peak gain of 42dB, in-band (IB) IIP3 of -33dBm at peak gain, and out-of-band (OOB) IIP3 of +19dBm when the circulator is in FD mode (Fig. 9.8.4). All these results are referred to the ANT port. The OOB IIP3 benefits from the filtering effect of the circulator's N-path filter at the RX input. The non-reciprocity between the ANT and TX ports is also shown in Fig. 9.8.4. The measured NF is 5.0dB in TDD RX mode, and increases to 8.4dB in FD mode due to circulator LO-path phase noise (Fig. 9.8.4). An integrated overall SI suppression of 42dB is achieved across the circulator and analog BB SIC over a BW of 12MHz (Fig. 9.8.5). Circulators require an impedance tuner to counter reflections due to antenna impedance mismatch. A tuner is used at the ANT port for joint-optimization of SIC BW between the circulator and the analog BB canceller. The analog BB SIC further increases the RX NF to 10.9dB. Figure 9.8.5 also depicts linearity tests under powerful SI. SIC of up to -4dBm of TX power results in small gain compression (~1dB) of a desired signal, as opposed to nearly 15dB of compression in the absence of analog BB SIC. Figure 9.8.5 also depicts both the main two-tone SI at the RX output as well as IM3 distortion generated on the SI by the circulator, RX and BB canceler for varying TX two-tone power. All signals are referred back to the ANT port to enable comparison with the noise floor of -92dBm. Analog BB SIC improves the effective in-band RX IIP3 from -33dBm to -18dBm. We have also implemented digital SIC in Matlab after capturing the baseband signals using an oscilloscope (an 8b quantizer). The digital SIC cancels not only the main SI but also the IM3 distortion generated on the SI. After digital SIC, the main SI tones are at the noise floor, while the SI IM3 tones are 8 dB below the noise floor for -7dBm TX average power. This corresponds to a total SI suppression of 85dB. The -7dBm TX average power is not limited by the circulator, but rather by the overall SI suppression achieved. Figure 9.8.6 compares this work to prior art. Key innovations include the integrated circulator with very low TX-ANT loss (1.7dB) and 85dB total SI suppression in conjunction with digital SIC.

Acknowledgement:
This work was supported by the DARPA ACT and RF-FPGA programs. The first two authors are equal contributors in this work.

References:
[1] D.-J. van den Broek et al., "A Self-Interference-Cancelling Receiver for In-band Full-Duplex Wireless with Low Distortion under Cancellation of Strong TX leakage," *ISSCC Dig. Tech. Papers*, pp. 344-345, Feb. 2015.
[2] J. Zhou et al., "Reconfigurable Receiver with >20MHz Bandwidth Self-Interference Cancellation Suitable for FDD, Co-Existence and Full-Duplex Applications," *ISSCC Dig. Tech. Papers*, pp. 342-343, Feb. 2015.
[3] D. Yang et al., "A Wideband Highly Integrated and Widely Tunable Transceiver for In-Band Full-Duplex Communication," *IEEE J. Solid-State Circuits*, vol. 50, no. 5, pp. 1189-1202, May 2015.
[4] M. Mikhemar et al., "A Multiband RF Antenna Duplexer on CMOS: Design and Performance," *IEEE J. Solid-State Circuits*, vol. 48, no. 9, pp. 2067-2077, Sept. 2013.

 978-1-4673-9467-3/16/$31.00

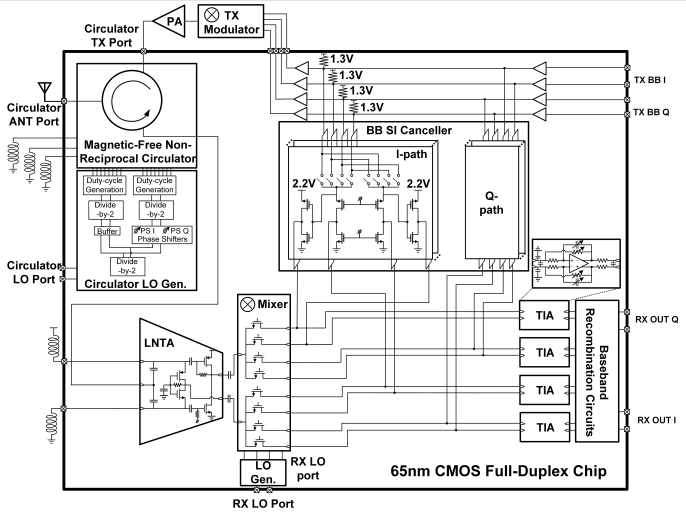

Figure 9.8.1: Proposed full-duplex receiver with integrated magnetic-free N-path-filter-based non-reciprocal circulator and analog baseband self-interference cancellation.

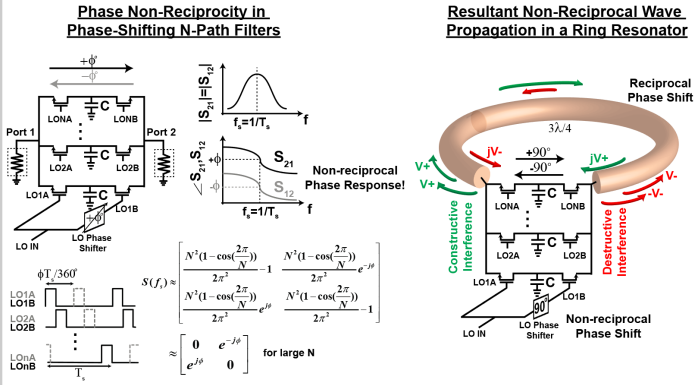

Figure 9.8.2: Magnetic-free non-reciprocity based on the non-reciprocal phase response of a two-port phase-shifting N-path filter, embedded within a 3λ/4 transmission-line ring.

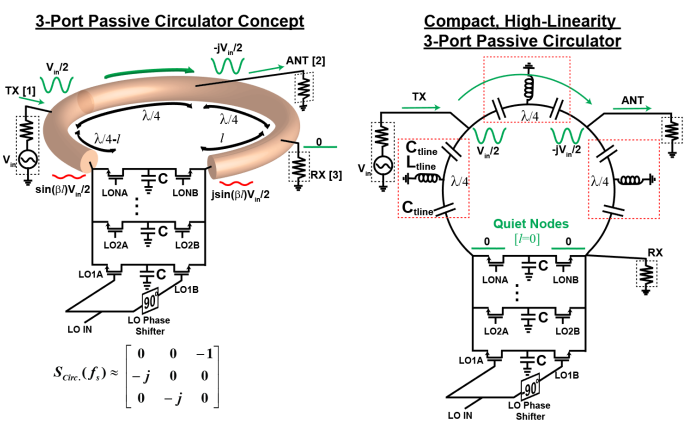

Figure 9.8.3: Evolution of the proposed high-linearity passive magnetic-free N-path-filter-based non-reciprocal circulator.

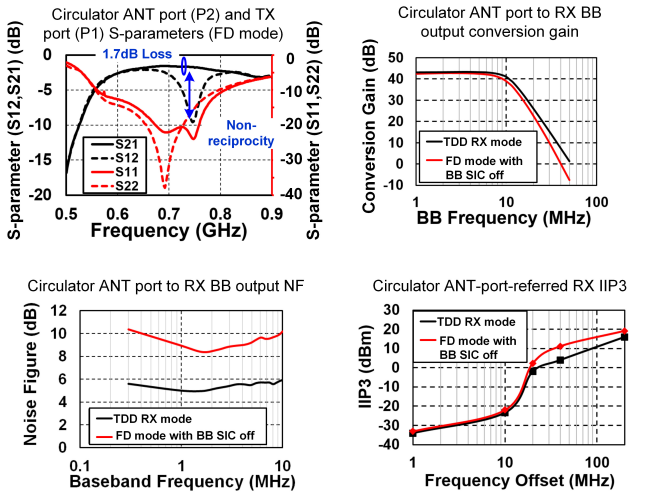

Figure 9.8.4: Measured circulator ANT-TX S-parameters in FD mode demonstrating non-reciprocity with only 1.7dB TX-to-ANT insertion loss, and circulator ANT-to-RX-BB characteristics.

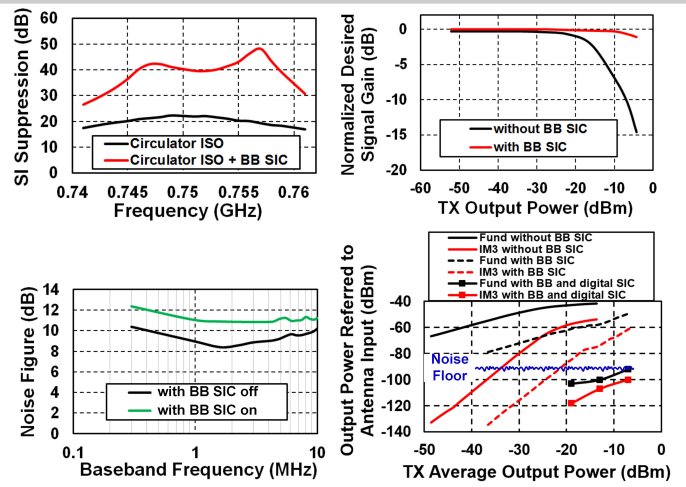

Figure 9.8.5: Measured small-signal SI suppression, impact of the BB SI canceller on RX NF in FD mode, gain compression of a weak desired signal with and without BB SIC, and two-tone linearity test with SI suppression across antenna, analog BB and digital domains.

	ISSCC 2015 [2]	ISSCC2015 [1]	JSSC 2015 [3]	This work
Architecture	RX with wideband SIC based on RF frequency-domain equalization	Mixer-first RX with SI-cancelling VM-downmixer	Mixer-first TRX with Active Baseband Duplexing	RX with integrated magnetic-free N-path-filter-based circulator and BB SIC
RX Frequency	0.8-1.4 GHz	0.15-3.5 GHz	0.1-1.5 GHz	0.6-0.8 GHz
Maximum Gain	42 dB	24 dB	53 dB	42 dB
Noise Figure	4.8 dB	6.3 dB	5-8 dB	5.0 dB (TDD mode)
OOB IIP3	+ 17 dBm	+22.0 dBm	+22.5 dBm	+19 dBm
IB IIP3	-20 dBm at 27 dB gain	+8 / +16.2 dBm at 24dB gain (Neg. conductance off/on)	-38.7 dBm at 53 dB gain	-33 dBm at 42 dB gain
Integrated Antenna Interface	No	No	Yes (baseband duplexing LNA)	Yes (magnetic-free non-reciprocal circulator)
Integrated SI Suppression Domains	RF	RF	Analog BB	Antenna + Analog BB
Amount of Integrated SI Suppression	20 dB SIC across 25 MHz BW	27 dB SIC across 16.25 MHz BW	33 dB across 300kHz TX BB BW	42 dB SIC across 12 MHz BW (incl. integrated circulator)
Effective IIP3 with respect to RX/ANT Input	+2 dBm at 27 dB gain	+19 dBm at 24dB gain	N/A	-18 dBm at 42 dB gain
Effective IIP3 with respect to TX Power	N/A	N/A	~0 dBm at 43/53 dB gain[1]	+1 dBm at 42 dB gain
NF Degradation in Full-Duplex Mode	0.9/1.3 dB[4]	4-6 dB[5]	N/R	6.5 dB[2] (incl. circulator in FD mode)
Overall SI Suppression	56 dB (incl. 34 dB isolation from antenna pair)	46 dB (incl. 25 dB isolation from antenna pair)[6]	N/A	85 dB (incl. digital SIC)
RX Power	63-69 mW	23-56 mW	43-56 mW (incl. TX)	60 mW signal path + 10 mW LO path (at 0.7GHz)
SI Canceller Power	0-182 mW			30 mW
Antenna Interface Power	N/A	N/A	N/A	59mW[3] (at 0.7GHz)
Technology	65 nm CMOS	65 nm CMOS	65 nm CMOS	65 nm CMOS
Active Area	4.8 mm²	2 mm²	1.5 mm²	1.4 mm²

1. From Fig. 31(a) in the paper. 2. Includes circulator 4.3dB NF, which is degraded from the expected 2dB NF due to LO phase noise. Elimination of the phase shifters (not necessary as only a static 90°phase shift is desired) restores the circulator NF to 2dB in simulation.
3. Circulator power consumption can be significantly reduced if the phase shifters are removed as only a static 90°phase shift is desired.
4. One/two canceller filters enabled. 5. Across VM settings. 6. From the follow-on JSSC paper. N/A: Not Applicable N/R: Not Reported

Figure 9.8.6: Performance summary and comparison.

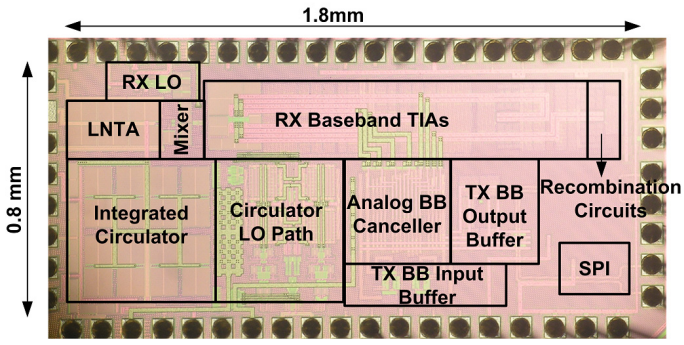

Figure 9.8.7: Die micrograph.

978-1-4673-9467-3/16/$31.00